Empirical specification of field-aligned plasma density profiles for plasmasphere refilling

Jiannan Tu,[1] Paul Song,[1] Bodo W. Reinisch,[1] James L. Green,[2] and Xueqin Huang[1]

Received 20 December 2005; revised 15 February 2006; accepted 22 March 2006; published 29 June 2006.

[1] Sounding measurements from the radio plasma imager (RPI) on the IMAGE satellite are used to derive electron density distributions along magnetic field lines in the nightside plasmasphere and plasmatrough for three midlatitude passes. These passes occurred during (1) a magnetic storm, (2) a prolonged quiet time, and (3) a sudden commencement of a storm, respectively. It is found that the density profiles of filled (in the inner plasmasphere) and depleted (in the plasmatrough or outer plasmasphere) flux tubes have different field line dependence. A multivariant least squares fit with a simple analytical function is used to model the density profiles. The fitting parameters in the function define the field line dependence of a density profile, i.e., the steepness of the density profile at high latitudes and the flatness at low latitudes. In each pass the density profiles along the filled and depleted flux tubes can be well modeled with the selected functional form, with two different sets of fitting parameter values for filled and depleted flux tubes. For the three passes examined, the fitting parameter values are not sensitive to the geomagnetic activity for the inner plasmasphere density profiles but vary slightly for the plasmatrough or outer plasmasphere density profiles from case to case. The equatorial densities extrapolated from the measured density profiles approximately have a power law relation with L values. The results suggest that the selected function has potential of being able to construct realistic global empirical plasmasphere/plasmatrough models. Furthermore, it is now feasible to empirically determine the density profiles along the depleted flux tubes for plasmasphere refilling studies.

Citation: Tu, J., P. Song, B. W. Reinisch, J. L. Green, and X. Huang (2006), Empirical specification of field-aligned plasma density profiles for plasmasphere refilling, *J. Geophys. Res.*, *111*, A06216, doi:10.1029/2005JA011582.

1. Introduction

[2] Realistic modeling of plasmasphere refilling is important for the understanding of plasmasphere dynamics and for space weather predictions. However, our ability to model the plasmasphere refilling processes is restricted by difficulty in specifying initial distributions of the plasma density, plasma flow velocity, and plasma temperatures along depleted magnetic flux tubes. In spite of several decades of efforts, we still have little knowledge about such initial plasma conditions. As a result of this limitation, the investigation of plasmasphere refilling is based on the initial conditions chosen by individual modelers. For example, a complete empty flux tube without any plasma content or a flux tube with an artificially specified initial density distribution has been used in simulating the plasmasphere refilling [e.g., *Banks et al.*, 1971; *Singh et al.*, 1986; *Rasmussen and Schunk*, 1988; *Wilson et al.*, 1992; *Liemohn et al.*, 1999; *Tu et al.*, 2003]. Nevertheless, aside from other factors, different initial flux tube density distribution may lead to different ion trapping mechanisms, i.e., distinct refilling scenarios at early stages of plasmasphere refilling [*Singh and Horwitz*, 1992]. Observations that measure the plasma distributions along depleted flux tubes are very valuable since they may specify initial conditions for plasmasphere refilling studies.

[3] The characteristics of depleted flux tubes can be obtained by examining the flux tubes in the nightside plasmatrough, particularly those close to the nightside plasmapause. This is because when the magnetospheric convection strength reduces, the corotation electric field may supersede the convection electric field at the locations of those flux tubes. Those flux tubes will then start corotating with the Earth, and refilling of plasma from the underlying ionosphere will occur. This concept has been used in calculations of the early and late time plasmasphere refilling rates at geosynchronous orbits [*Lawrence et al.*, 1999; *Su et al.*, 2001]. The flux tubes in the outer plasmasphere near the nightside plasmapause may be regarded as depleted flux tubes as well, if the plasma densities within them are substantially below the filled plasmasphere density level. Such flux tubes are equivalent to flux tubes at the early stages of the plasmasphere refilling.

[4] Studies on the electron density in the plasmatrough have been conducted previously. *Carpenter and Anderson* [1992] developed an empirical model for the equatorial

[1]Center for Atmospheric Research, University of Massachusetts-Lowell, Lowell, Massachusetts, USA.
[2]NASA Goddard Space Flight Center, Greenbelt, Maryland, USA.

0148-0227/06/2005JA011582

electron density in the plasmasphere and plasmatrough. They showed that the equatorial density in the plasmatrough, on the average, varies as $L^{-4.5}$, where L is the apex of a geomagnetic field line in Earth's radius R_E. Several similar empirical relations have been developed in recent years based on plasmaspheric and plasmatrough density observations [*Gallagher et al.*, 2000; *Goldstein et al.*, 2001; *Sheeley et al.*, 2001; *Denton et al.*, 2002, 2004]. In principle one may obtain the field line dependence of the plasma densities (i.e., the density distribution along the field line) through statistically averaging of a large set of measurements but as such this procedure does not represent the actual field line density distribution at a given time. So far the field line dependence is derived from the average electron densities measured in coarse coverage of L shells and latitudes [e.g., *Gallagher et al.*, 2000; *Goldstein et al.*, 2001; *Denton et al.*, 2002, 2004]. In addition, the plasma distribution may vary substantially both in space and time during magnetic storms, compromising the values of statistical models. Therefore instantaneously measuring the electron density distribution along a magnetic field line is necessary in order to accurately determine the plasma density and its field line dependence along a depleted flux tube.

[5] Recently, the radio plasma imager (RPI) [*Reinisch et al.*, 2000] on the IMAGE satellite [*Burch et al.*, 2001] has provided nearly instantaneous measurements of the electron density distribution along a magnetic field line [*Reinisch et al.*, 2001]. A nearly instantaneously measured field-aligned density profile specifies the field line dependence of the electron densities in an extended latitude range along the field line at the time of measurement. This allows precise modeling of the field line dependence along an entire magnetospheric field line based on the density variations of the measured density profile. Such measurements have been used to successfully construct empirical models of electron densities for the noon and morning sectors of the plasmasphere [*Reinisch et al.*, 2004; *Huang et al.*, 2004; *Song et al.*, 2004].

[6] The purpose of this paper is to apply a similar functional form used in the above RPI studies to empirically model the field-aligned density distributions in the nightside plasmasphere and plasmatrough. We will show that this functional form can represent well not only the density profiles in the dayside plasmasphere but also the density profiles along the filled and depleted flux tubes on the nightside. Therefore this functional form has potential of being used to develop global empirical models of the plasmasphere/plasmatrough. In particular, it can be used to provide initial flux tube density profiles for studying the plasmasphere refilling because the flux tubes in the plasmatrough may begin to corotate with the Earth when the magnetospheric convection decreases.

2. Measurements and Density Inversion Technique

[7] The design and measurement characteristics of the radio plasma imager (RPI) on the IMAGE satellite have been described in detail by *Reinisch et al.* [2000] and the inversion technique for obtaining field-aligned density profiles has been discussed in previous studies [*Reinisch et al.*, 2001, 2004; *Huang et al.*, 2004]. In brief, the RPI, in active sounding modes, transmits coded signals at varying frequencies from 3 kHz to 3 MHz and listens to the echoes. The received echoes are plotted in a ''plasmagram'', a color-coded display of signal amplitude as a function of frequency and echo delay time (represented as virtual range: the echo delay time multiplied by one half of the vacuum speed of light). Multifrequency echoes can form a distinct trace in a plasmagram. It has been shown that under certain conditions, the traces represent the reflected signals that propagate along a magnetic field line threading the satellite [see *Reinisch et al.*, 2001; *Fung and Green*, 2005]. Applying a standard density inversion algorithm [*Huang et al.*, 2004], we can derive a density distribution along a field line almost instantaneously (in < 1 min). In passive observation modes, the RPI receives natural plasma waves. These natural plasma wave signals are displayed in conventional frequency-time spectrograms [*Green and Reinisch*, 2003]. The passive and active modes are operated alternately.

3. Modeling Density Profiles of Nightside Flux Tubes

[8] In this section we examine and model field-aligned density profiles derived from the RPI active sounding measurements during three IMAGE passes of the plasmasphere and plasmatrough around the local magnetic midnight. We apply a functional form to model those density profiles separately for each pass. The functional form used in the present study is similar to that developed by *Huang et al.* [2004] and *Song et al.* [2004]

$$N_e = N_0(L)\cos^{-\beta(L)}\left(\frac{\pi}{2}\frac{\alpha(L)\lambda}{\lambda_{in}}\right)$$
$$\alpha(L) = A + B\cdot L,\ \beta(L) = C + D\cdot L, \tag{1}$$

where λ and λ_{in} are the magnetic latitude along a field line and the invariant latitude of the field line, respectively, $N_0(L)$ is the minimum electron density of the RPI measured density profiles, which is the in situ electron density at the satellite location in the cases examined in following subsections. Parameter $\alpha(L)$ describes the steepness of the density profiles at high latitudes, while $\beta(L)$ specifies the flatness of the profiles at low latitudes. The fitting parameters A, B, C, and D are to be determined by multivariant least squares fit to the density profiles derived from the RPI sounding measurements along each of the three IMAGE passes. The multivariant least squares fit requires that the square sum of the difference between the measured and modeled densities is minimized with respect to four common fitting parameters

$$\Delta = \sum_i \sum_j \left[N^*_{eij} - N_{eij}\right]^2 = \min, \tag{2}$$

where i and j represent the ith field line and the jth point on the ith field line, respectively, N^*_{eij} and N_{eij} are the measured and modeled electron density, respectively.

[9] *Huang et al.* [2004] have shown that this function, with appropriate values of fitting parameters, does well represent the measured density profiles along field lines

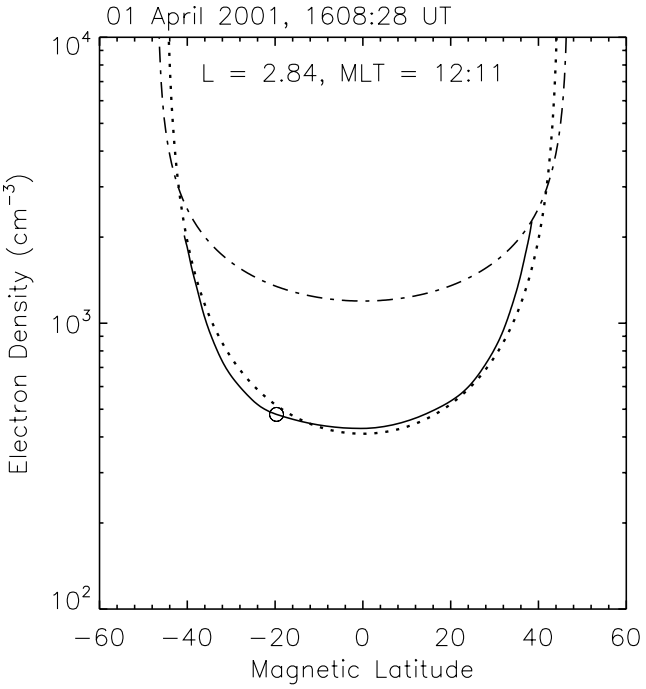

Figure 1. Field-aligned electron density profile (solid line) derived from the RPI sounding measurements during a magnetic storm on 1 April 2001. The circle shows the latitude of the satellite on the field line. The dashed-dotted line is the quiet time density profile from the empirical model of *Reinisch et al.* [2004]. The dotted line is the least squares fit to the measured density profile using equation (1).

from the southern to northern hemisphere in the filled noon and morning plasmasphere [*Reinisch et al.*, 2004; *Song et al.*, 2004]. We will show that this function can as well be used to model the density profiles of depleted plasmaspheric flux tubes. We take the density profile (solid line) in Figure 1, derived from the RPI sounding measurements during a magnetic storm, on 1 April 2001, as an example. By comparing with the quiet time density profile (dashed-dotted line) given by the empirical plasmasphere model of *Reinisch et al.* [2004] (with $A = 1.25$, $B = 0$, $C = 0.2$, $D = 0.03$, and $N_0 = 1195.3$ cm^{-3}) for the same field line, we can conclude that the RPI measured density profile is for a depleted flux tube. The dotted line in Figure 1 is the least squares fit to the measured density profile using equation (1) with $N_0 = 410.5$ cm^{-3} and the fitting constants $A = 0.99$, $B = 0.09$, $C = 0.6$, $D = 0.1$. It is seen that the fitting function models the depleted density profile quite well. We conclude that this functional form is sufficiently flexible to describe both the filled and depleted density profiles on the dayside. Next, we will show that it can also represent the field-aligned density profiles along the filled and depleted flux tubes on the nightside.

[10] In Figure 1, and in previous studies that used the functional form given in equation (1) to model the plasmasphere density distributions [*Reinisch et al.*, 2004; *Huang et al.*, 2004; *Song et al.*, 2004], the equatorial density N_{eq} and the densities near the equator are constrained by the measured density profiles. In those previously examined cases, the RPI density profiles along the field lines were derived from one hemisphere to another because each plasmagram contains at least two traces. One trace was formed by echoes reflected from altitudes lower than that of the satellite in the local hemisphere along the field line. Another trace represented signals along the same field line but reflected from the conjugate hemisphere. The waves in the latter trace must have traveled across the equatorial region along the field line [*Reinisch et al.*, 2001]. No signals are reflected from the equatorial region where the electron densities are lower than that at the satellite location. The first echo (with the lowest frequency) on the conjugate trace comes from the conjugate point where the density is the same as that at the satellite. The total electron content in the equatorial region is known from the time delay of the conjugate lowest frequency echo. On the basis of the assumption that the density gradients are continuous, the densities in the equatorial region (including the equatorial density) are interpolated with the constraint of the known total electron content in that region [*Huang et al.*, 2004]. When IMAGE crosses the magnetic equator, the RPI can measure the equatorial density directly, at least at one L shell. In the present study, the plasmagrams taken by the RPI at $L > 2.7$ on the nightside contain only the trace from the local hemisphere. Each density profile in this study is then derived for only the local hemisphere segment of the field line. The electron densities in the equatorial region beyond the latitude range of the RPI density profile, including equatorial density, are not directly derived from the RPI measurements but extrapolated through the multivariant least squares fit.

[11] The RPI measured density profiles examined in the present study were obtained from 0119:03 to 0143:03 UT on 22 March 2001, from 0533:06 to 0557:06 UT on 5 November 2004, and from 1417:06 to 1435:06 UT on 7 November 2004. The first period was during the recovery phase of a magnetic storm when the hourly Dst = −48 nT, while the second one was in the last day of a 5-day quiet period. Kp index was 1 when the RPI measurements were made on 5 November 2004 and primarily less than 3 in the preceding 5 days. The third period was during a sudden commencement (Dst = 37 nT) of a great magnetic storm. The sudden commencement started about 3 hours before the RPI measurements. These three cases demonstrate three representative plasmasphere-plasmatrough (or outer plasmasphere) transitions observed by the IMAGE RPI. Table 1 shows the times and locations at which the plasmagrams were obtained by the RPI. In this study the L shell of a field line is defined as the apex of the field line (in unit of the Earth's radius R_E), calculated using the Tsyganenko 2001 (T01) [*Tsyganenko*, 2002] magnetospheric magnetic field model. The invariant latitude, λ_{in}, is defined as the average of the magnetic latitudes of the footprints (on the ground) of the calculated field line in the two hemispheres. The invariant latitude is a parameter used in the fitting function in order to properly limit the modeled field-aligned density profile to below the maximum magnetic latitudes of the field line. Other definitions, such as the dipole invariant latitude defined by $\cos^2(\lambda_{in}) = 1/L$ can also be used. Using the other definitions of the invariant latitude will, however, result in different values of the fitting parameters A and B for a given measured density profile because the condition

Table 1. UT, Invariant Latitude, Magnetic Latitude, *L* Shell, and MLT of the RPI Measurements on 22 March 2001, 5 and 7 November 2004

	UT	ILAT	MLAT	*L*	MLT
			22 March 2001		
1	0119	48.3°	13.3°	2.23	0059:18
2	0123	51.6°	18.3°	2.48	0103:00
3	0127	54.8°	22.7°	2.78	0106:30
4	0131	57.8°	26.7°	3.15	0109:49
5	0135	60.5°	30.2°	3.59	0113:08
6	0143	65.2°	36.4°	4.89	0119:10
			5 November 2004		
1	0533	47.7°	−19.3°	2.22	2255:08
2	0536	50.5°	−23.8°	2.50	2258:59
3	0539	53.2°	−27.8°	2.82	2302:57
4	0542	55.7°	−31.4°	3.20	2306:23
5	0545	58.0°	−34.7°	3.65	2309:15
6	0548	60.0°	−37.7°	4.19	2312:19
7	0551	61.9°	−40.5°	4.83	2315:17
8	0554	63.7°	−43.0°	5.65	2318:27
9	0557	65.3°	−45.5°	6.79	2321:25
			7 November 2004		
1	1417	35.7°	−14.3°	1.65	2235:45
2	1420	40.2°	−21.4°	1.92	2235:22
3	1423	44.6°	−27.7°	2.28	2234:38
4	1426	48.6°	−33.3°	2.76	2233:49
5	1429	52.3°	−38.2°	3.36	2232:54
6	1432	55.6°	−42.5°	4.11	2232:08
7	1435	58.5°	−46.5°	5.03	2231:25

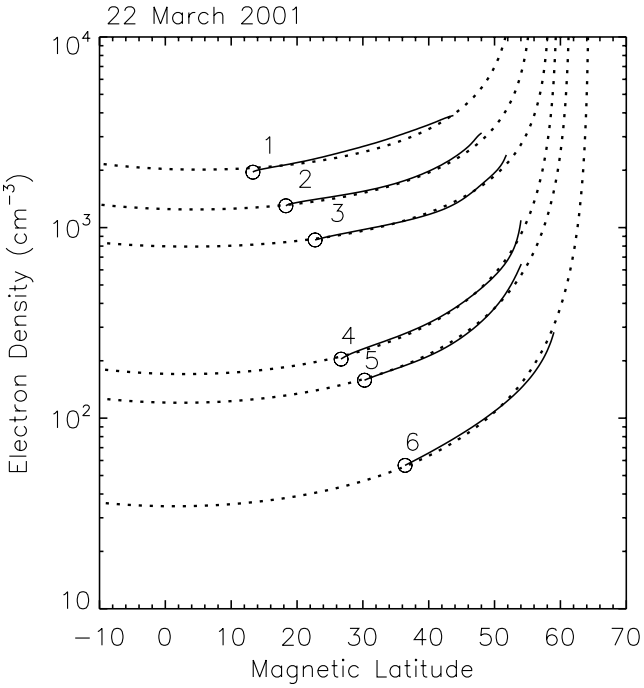

Figure 2. Field-aligned electron density profiles derived from the RPI sounding measurements made from 0119:03 to 0143:03 UT on 22 March 2001. The circle on each profile indicates the satellite location. Profile number is labeled beside each profile. The dotted lines are the multivariant least squares fits to the measured density profiles using equation (1).

$\alpha(L)\lambda/\lambda_{in} < 1$ must be satisfied in equation (1). Note that equation (1) is applicable to model plasmasphere electron density distributions but not to underlying ionosphere density distributions because the functional form was derived from the measurements of field-aligned density profiles in the plasmasphere.

3.1. Case of 22 March 2001 (Storm Recovery Phase)

[12] We first consider the RPI measurements made from 0119:03 to 0143:03 UT on 22 March 2001. Figure 2 displays the density profiles derived from the RPI measurements for this case (solid lines). The circle at the bottom of each density profile indicates the satellite latitude at the time of the measurement. In Figure 2 as well as later in Figures 6 and 9, the profile number is in sequence of increasing *L* shell (see Table 1). It is noted that the measured density profiles 1–3 in Figure 2 have a slope that is significantly different from the slope of profiles 4–6: the densities of the outer three profiles increase faster with latitude along the field lines. This suggests that in order to obtain the best agreement between the measured and modeled density profiles, we need to perform multivariant least squares fits separately for these two groups of density profiles. The results of the two separate multivariant least squares fits to the two profile groups are plotted as dotted lines in Figure 2, which show good agreement with the measured profiles for both groups. The values of the constants *A*, *B*, *C*, and *D*, for profiles 1–3 and profiles 4–6, are listed in Table 2. Also listed are the extrapolated equatorial densities N_{eq} for all the measured density profiles. The standard deviation of the extrapolated equatorial density is estimated to be less than 20% for the dayside density profiles [*Reinisch et al.*, 2004]. This standard deviation, 20%, may be also applicable to the nightside density profiles. However, it is needed to be confirmed by using equatorial densities actually measured on the nightside, which are not found in the RPI measurements so far. The resultant parameter $\alpha(L)$ is independent of *L* for profiles 1–3 (the constant $B = 0$) but weakly ($B \neq 0$ but small) dependent on *L* for profiles 4–6. The major difference occurs in the values of constants *C* and *D* for the two groups. If we used the same values of *C* and *D* for both groups, one group of density profiles would be poorly fit, depending on which set of values of *C* and *D* are used.

[13] The difference in the field line dependence of the two density profile groups suggests that they were measured in distinctly different plasma regions, namely, plasmasphere and plasmatrough. Figure 3 is the plot of the electron densities along the IMAGE orbit. The in situ measured density reveals a decrease when the satellite moved outward from the plasmasphere. Particularly, there is a steep density drop from 0127 to 0131 UT (from $L = \sim 2.8$ to ~ 3.2). This

Table 2. Values of Fitting Parameters *A*, *B*, *C*, and *D*, and the Extrapolated Equatorial Densities N_{eq} (cm^{-3}) for the Density Profiles on 22 March 2001

	UT	*L*	N_{eq}	*A*	*B*	*C*	D
1	0119:03	2.23	2015.2				
2	0123:03	2.48	1245.4	0.999	0	0.45	0.055
3	0127:03	2.78	795.1				
5	0131:03	3.15	170.4				
6	0135:03	3.59	120.5	0.99	0.009	0.6	0.1
7	0143:03	4.89	34.5				

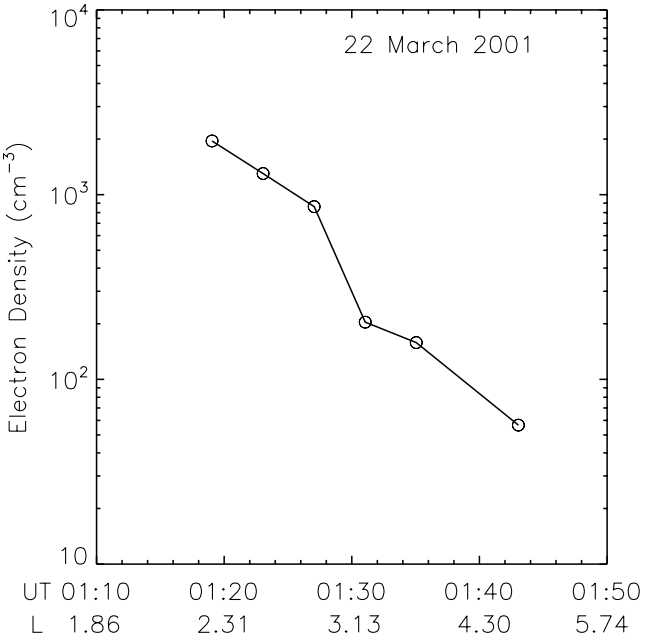

Figure 3. Electron density along the IMAGE trajectory from the RPI active sounding measurements from 0119:03 to 0143:03 UT on 22 March 2001. *L* values are also marked under abscissa.

density variation along the satellite trajectory is verified by examining the upper hybrid resonance (UHR) noise band observed in RPI passive mode measurements. The UHR noise is a narrow band of electrostatic waves bounded by the local hybrid resonance frequency (f_{uh}) and electron plasma frequency (f_{pe}) [e.g., *Mosier et al.*, 1973; *Benson et al.*, 2004]. The RPI dynamic spectrum for the interval of 0030–0230 UT on 22 March 2001 in Figure 4, clearly shows the expected UHR band enhancement. The UHR frequency experiences a sharp decrease from ~0125 UT to ~0132 UT, roughly coincident with the steep density gradient in Figure 3 derived from RPI active measurements. Since IMAGE moved radially outward as well as toward higher latitudes, the density variation along the IMAGE orbit is due to the combined effects of the radial distance and latitude increases. While the density decreases when moving radially outward, the density should increase when moving to higher latitudes along a given field line, which to some degree compensates for the density decrease due to the radially outward motion in this case. Thus we conclude that the steep density gradient along the satellite trajectory really indicates crossing of a boundary, i.e., the plasmapause. Therefore the density profiles 1–3 and 4–6 are indeed measured in different plasma regions, i.e., in the plasmasphere and plasmatrough, respectively.

[14] The multivariant least squares fit results in a model function that reproduces the measured density profiles very well, as demonstrated by Figure 2. However, as indicated

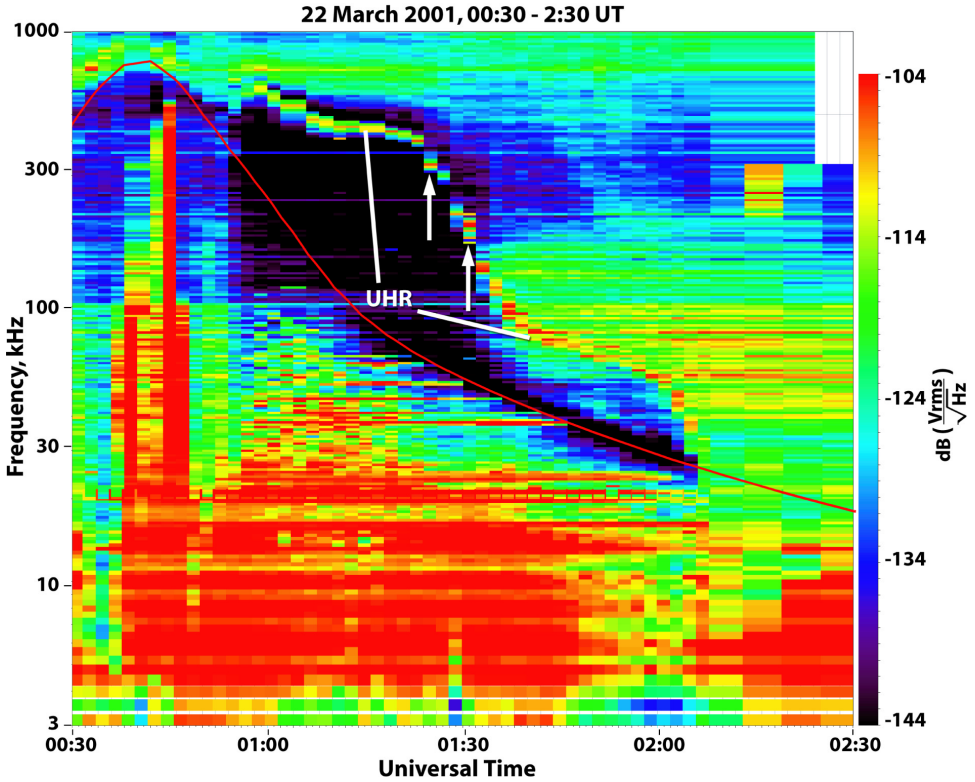

Figure 4. Dynamic spectrum obtained by the RPI during the interval of 0030–0230 UT on 22 March 2001. A UHR noise band is clearly displayed. The frequency of the band decreases sharply from about 0126 UT to 0132 UT, as indicated by two arrows. The red line is electron cyclotron frequency calculated from T01 [*Tsyganenko*, 2002] magnetospheric magnetic field model.

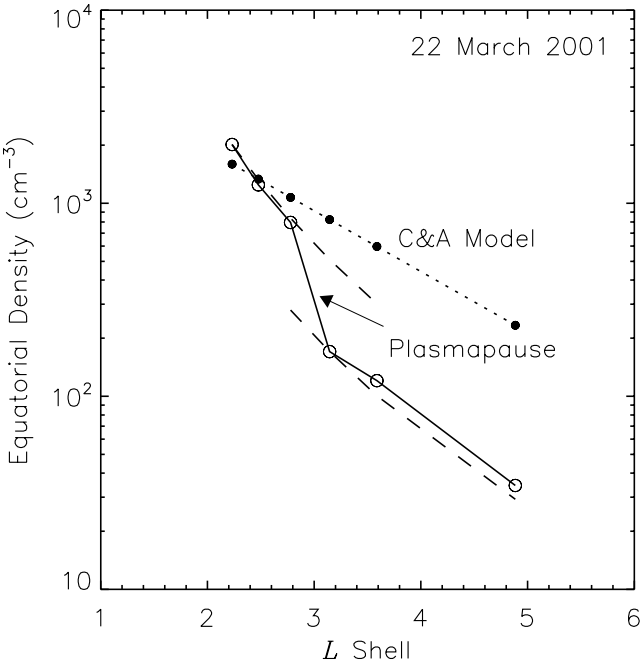

Figure 5. Equatorial density extrapolated from the multivariant least squares fits to the measured density profiles for the 22 March 2001 case (solid line with open circles). The two segments of the dashed lines are L^{-4} dependence for the equatorial density in the plasmasphere and plasmatrough, respectively. The dotted line with filled circles is the filled plasmasphere equatorial density from the *Carpenter and Anderson* [1992] model.

previously, the density distributions beyond the latitude range of the measured density profiles are extrapolated rather than directly derived from the RPI measurements. By examining the characteristics of the equatorial densities extrapolated from the multivariant fit, we may to some degree verify that the extrapolation is reasonable. In Figure 5 we plot the L dependence of the extrapolated equatorial density. The two dashed lines represent a L^{-4} dependence of the equatorial densities in the plasmasphere and plasmatrough, respectively. The dotted line with filled circles is the filled plasmasphere density from the *Carpenter and Anderson* [1992] model. There is a steep gradient in the extrapolated equatorial density from $L = \sim 2.78$ to ~ 3.15, with the density dropping about 80% within $\sim 0.37\ R_E$. The location of this steep density gradient, or the plasmapause, is the same as the plasmapause location identified from the variations of the in situ measured electron density. Furthermore, the extrapolated equatorial density follows the L^{-4} dependence in both the plasmasphere and plasmatrough. The L dependence of the extrapolated plasmatrough equatorial densities is flatter than that of the plasmatrough equatorial densities from *Carpenter and Anderson* [1992] empirical model (there $N_{eq} \propto L^{-4.5}$), and the plasmasphere equatorial densities presented here decrease with L faster than those given by that empirical model (dotted line in Figure 5). In comparison, previous case observations [e.g., *Angerami and Carpenter*, 1966; *Reinisch et al.*, 2004] showed the L^{-4} dependence of the equatorial densities in the plasmasphere and plasmatrough. Therefore the equatorial densities extrapolated from the multivariant best fit are not inconsistent with the previous observations. This gives us some confidence that the extrapolation of the measured density profile to the latitudes beyond the latitude range of the measurements is reasonable. Nevertheless, we should keep in mind that there is some uncertainty in the equatorial values due to the extrapolation.

3.2. Case of 5 November 2004 (Prolonged Quiet Period)

[15] In Figure 6 we plot the field-aligned density profiles derived from the RPI measurements during 0533:06–0557:06 UT on 5 November 2004 (refer to Table 1 for the times and locations of the RPI measurements). In this case, the field line dependence of the density profiles is more complicated. First, the profiles 2–3 are flatter than the profile 1 and profiles 4–6. Second, the outermost three profiles have steeper slopes than the other profiles. Therefore we should apply the multivariant least squares fit to multiple groups of density profiles. From the best fit we find that the field line dependence of the profile 1 is also unique: it cannot be well fitted using any set of fitting parameters A, B, C, and D suitable to other three groups (profiles 2–3, 4–6, and 7–9), i.e., it must be fitted individually. The best-fit density profiles are overplotted in Figure 6 as dotted lines. The fitting constants A, B, C, and D are given in Table 3. The two sets for the outer six profiles just resemble those in 22 March 2001 case: one set for plasmasphere density profiles with the same values of the fitting constants as those in 22 March 2001 case, and one set for plasmatrough-like profiles with slightly different values of constants A and D from those in the previous case (compare Table 2 and 3).

[16] This case demonstrates that the density variations along the field lines on low L shells can be quite compli-

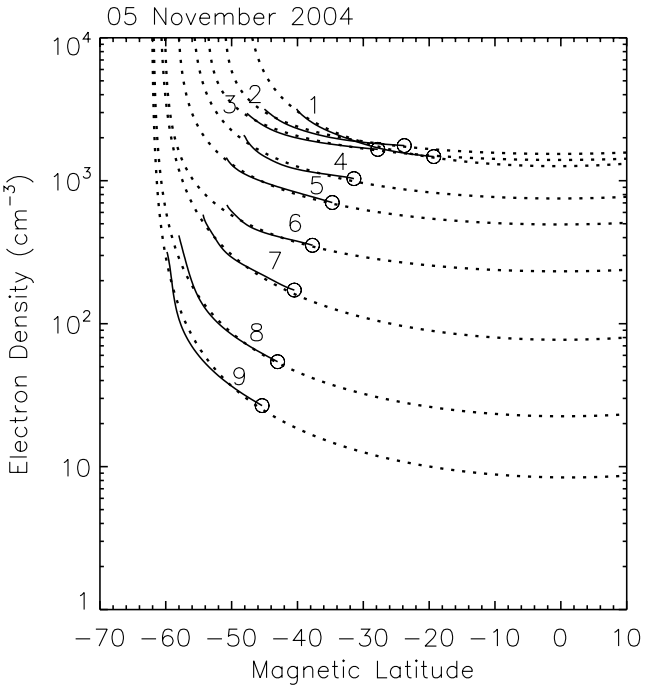

Figure 6. The same format as Figure 2 but for the density profiles in the 5 November 2004 case.

Table 3. Same Format as Table 2 but for 5 November 2004 Case

	UT	L	N_{eq}	A	B	C	D
1	0533:06	2.22	1265.1	0.999	0	0.45	0.1
2	0536:06	2.50	1540.8	0.997	0	0.36	0.02
3	0539:06	2.82	1398.2				
4	0542:06	3.20	751.3				
5	0545:06	3.65	494.6	0.999	0	0.45	0.055
6	0548:06	4.19	232.4				
7	0551:06	4.83	77.2				
8	0554:06	5.65	22.5	0.97	0.009	0.6	0.09
9	0557:06	6.79	8.4				

cated even during prolonged quiet period (note that this case was during the last day of a 5-day quiet period). Owing to the complexity of profiles 1–3, the extrapolated equatorial densities display an interesting feature, namely a density plateau around $L = 2.5$ in Figure 7, a plot of the extrapolated equatorial density as a function of L. The equatorial density then rapidly decreases outward after the density plateau. Actually, the in situ density along the IMAGE orbit also displays a density plateau around about $L = 2.5$, as shown in Figure 8. Such density variation resembles density profile pattern B observed by *Horwitz et al.* [1990] using in situ data from the DE-1 satellite (see Figure 1 of their paper).

[17] In this pass it appears that the plasmasphere extends to at least $L \sim 7$ on the nightside without the signatures of the plasmapause. This is consistent with the variation of the UHR frequency in the dynamic spectrum (not shown here) for this pass through the plasmasphere. The frequency of the UHR band kept decreasing when the IMAGE satellite moved outward from the plasmasphere.

[18] The dashed line in Figure 7 represents a L^{-4} dependence of the equatorial density. It is seen that the equatorial density in the inner plasmasphere (except the density plateau) decreases as L^{-4}. However, the outer plasmasphere (the outermost three density profiles at $L \geq 4.8$) equatorial density decreases with L faster than L^{-4} and is approximately $\propto L^{-6}$ (dashed-dotted line). In addition, the outer plasmasphere is far from reaching filled state: the extrapolated equatorial density at $L = 6.79$ (close to geosynchronous orbit at 6.6 R_E) is only 8.4 cm^{-3}, much less than the filled equatorial density of ~50–100 cm^{-3} at that altitude [e.g., *Sojka and Wrenn*, 1985; *Carpenter and Anderson*, 1992; *Lawrence et al.*, 1999]. In Figure 7 we also plot the filled equatorial density predicted by the *Carpenter and Anderson* [1992] model (dotted line with filled circles), which gives a equatorial density at $L = 6.79$ about one order of magnitude larger than that extrapolated from the fit to the RPI measured density profiles. Thus the flux tubes around $L = 6.79$ are categorized as depleted flux tubes. It is possible that they are at the early stages of the refilling [e.g., *Lawrence et al.*, 1999]. As indicated previously, the magnetic activity was quiet for about 5 days prior to the RPI measurements. It is not clear how the nightside flux tubes at $L \geq 4.8$ kept depleted for several days. A number of substorms during 3–4 November (as displayed by AE index variations, not shown) might be the cause but we cannot confirm it with the current data set. The inner flux tubes may represent filled plasmaspheric flux tubes since their equatorial densities are comparable to those from the *Carpenter and Anderson* [1992] model for filled plasmasphere.

3.3. Case of 7 November 2004 (Storm Sudden Commencement)

[19] Figure 9 shows the density profiles derived from the RPI measurements during 1417:06–1435:06 UT on 7

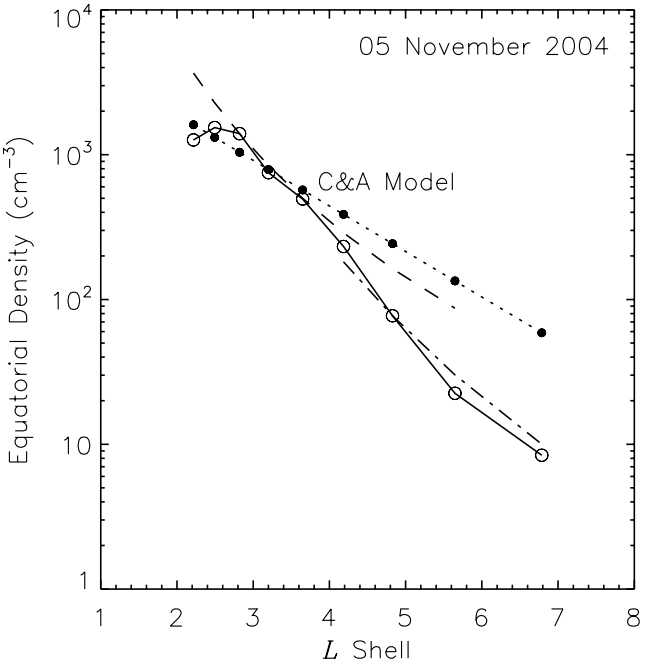

Figure 7. The same format as Figure 5 but for the 5 November 2004 case. The dashed line and dashed-dotted line is L^{-4} and L^{-6} dependence of the equatorial density, respectively.

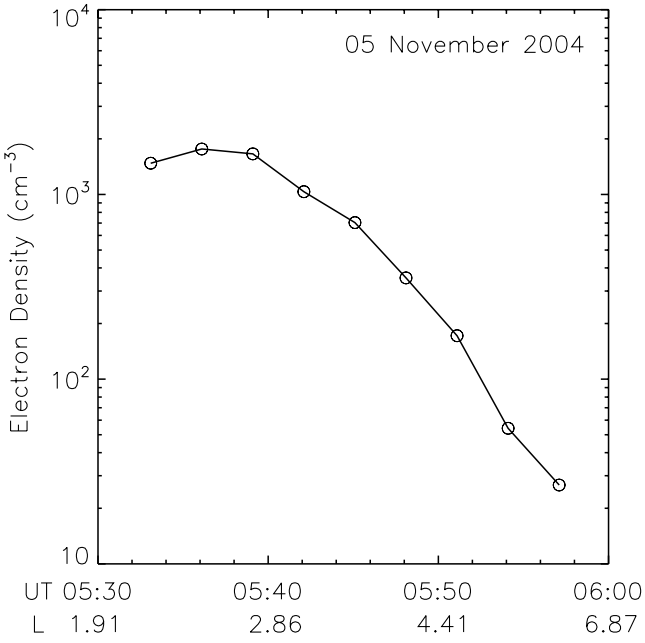

Figure 8. Electron density along the IMAGE trajectory from the RPI sounding measurements from 0533:06 to 0557:06 UT on 5 November 2004. L values are also marked under abscissa.

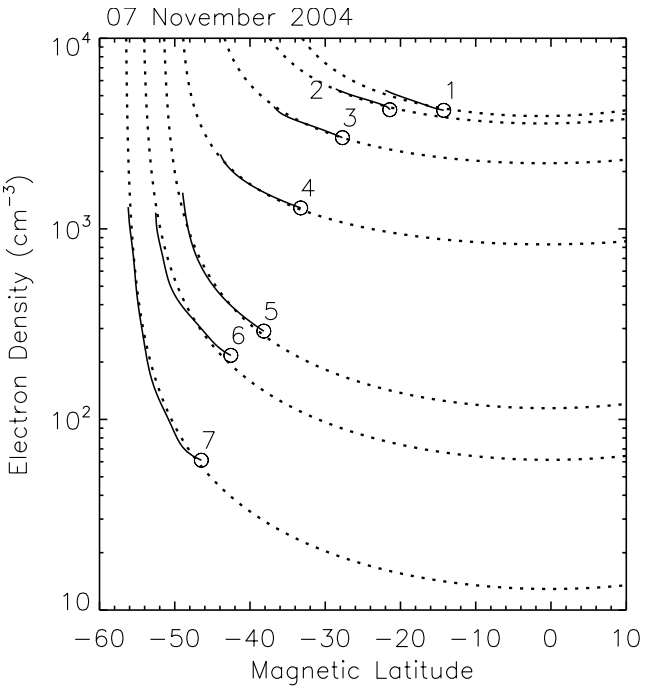

Figure 9. The same format as Figure 2 but for the density profiles in the 7 November 2004 case.

November 2004. We can see that the outermost three density profiles are of different field line dependence from the inner four profiles: they have steeper slopes. Therefore two sets of multivariant least squares fits are applied, separately for these two groups of density profiles. The best-fit density profiles are overplotted in the figure, with the values of the fitting parameters given in Table 4. The fitting constants A, B, and C are of the same values as the 22 March 2001 values except that the value of D for the outer three density profiles (profiles 6–7) is slightly different from that for profiles 4–6 of the 22 March 2001 case.

[20] The variation of the extrapolated equatorial density with L in this case, displayed in Figure 10, is similar to that in the 5 November 2004 case but the equatorial density monotonically decreases with L without density plateau. The extrapolated equatorial density slightly levels up at $L \geq 3.36$ and the in situ density (not shown here) displays similar variation. Such variation perhaps is the signature of the plasmapause but the density gradient is not large enough to definitely identify the location of the plasmapause. Nevertheless, one point is clear: The extrapolated equatorial density of the flux tubes in the region of $L \geq 3.36$ is about one order of magnitude smaller than that predicted by the *Carpenter and Anderson* [1992] model (dotted line in Figure 10), suggesting that those flux tubes are depleted flux tubes and are at the early refilling stages. Again the inner flux tubes may be in filled states because their equatorial densities are comparable to those from the empirical model of *Carpenter and Anderson* [1992]. It is also interesting to note that the equatorial density in the inner plasmasphere has an approximate L^{-4} dependence (dashed line) and varies approximately as $L^{-5.1}$ in the outer plasmasphere (dashed-dotted line).

Table 4. Same Format as Table 2 but for 7 November 2004 Case

	UT	L	N_{eq}	A	B	C	D
1	1417:06	1.65	3909.5				
2	1420:06	1.92	3574.9	0.999	0	0.45	0.055
3	1423:06	2.28	2210.3				
4	1426:06	2.76	829.4				
5	1429:06	3.36	114.6				
6	1432:06	4.11	61.4	0.99	0.009	0.6	0.11
7	1435:06	5.03	12.9				

4. Discussion and Conclusions

[21] We have presented three periods of the RPI observations made in the nightside plasmasphere and plasmatrough. These cases demonstrate representative plasmasphere-plasmatrough transitions of the IMAGE satellite around local midnight: during a magnetic storm, prolonged quiet time, and the sudden commencement of a magnetic storm. We examined the field line dependence (i.e., the field-aligned variations) of the densities on those profiles and use a simple functional form to model the field line dependence. It is found that in each case the measured field-aligned density profiles in the outer plasmasphere or in the plasmatrough display a steeper slope than those in the inner plasmasphere, i.e., different field line dependence. The density profiles in the inner plasmasphere, except the complicated density structures of the 5 November 2004 case, have the same field line dependence so that they can be well represented by the functional form of equation (1) with the same set of fitting parameter values for all three cases. Because of the differences in the field line dependence, the density profiles in the plasmatrough or outer depleted plasmasphere are modeled by the equation (1) with fitting

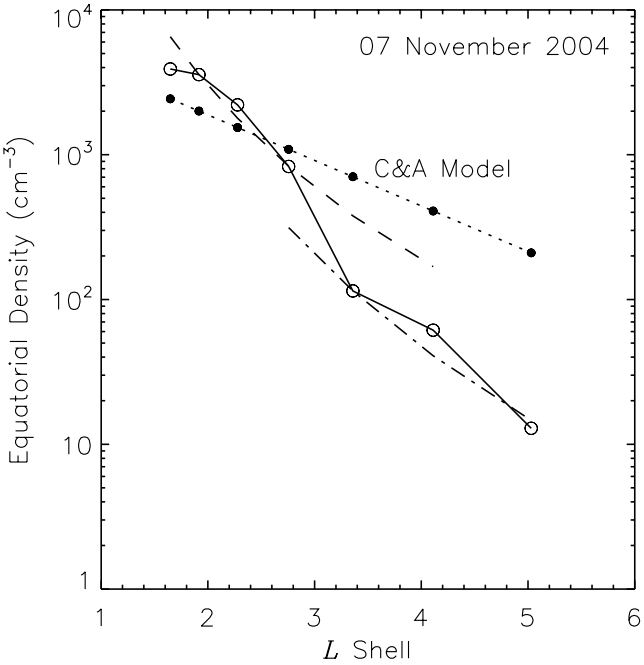

Figure 10. The same format as Figure 7 but for the 7 November 2004 case. The dashed line and dashed-dotted line is L^{-4} and $L^{-5.1}$ dependence of the equatorial density, respectively.

parameter values different from those for the inner plasmasphere density profiles. In addition, the values of those fitting parameters for the density profiles in the plasmatrough or outer plasmasphere vary slightly from case to case, possibly indicating the variation of the field line dependence of the depleted flux tube densities in association with the geomagnetic variations and other factors such as season and refilling stages.

[22] As shown in Tables 2–4, the values of the parameter A is essentially equal to 1 and $B = 0$ in the inner plasmasphere for all the three cases. Therefore we may simply take $\alpha = 1$ for the inner filled plasmasphere. However, since B and D is multiplied by L in parameter α and β, a slight change of their values may result in significant variations in values of α and β in the region of large L. Such variations in values α and β will give rise to notable change of the density slope defined by cosine function in equation (1). Keeping nonzero B and D in α and β is thus necessary and their small changes have significant effects on the modeled density profiles from case to case in the region of large L.

[23] It has been shown in previous studies that the functional form of equation (1) well represented the field-aligned density profiles in the filled plasmasphere [*Huang et al.*, 2004; *Reinisch et al.*, 2004; *Song et al.*, 2004]. It is further demonstrated in the present study that it also well suits to model the field-aligned density profiles along both the filled and depleted flux tubes around local midnight. This functional form thus has the potential to be used for constructing global empirical plasmasphere/plasmatrough models. Particularly, it is feasible to be used to specify the density profiles along the nightside depleted flux tubes for the studies of plasmasphere refilling with appropriately specified fitting constant values and equatorial densities.

[24] The cases shown in the present paper suggest that there are two different field line dependence of the field-aligned density profiles in the inner filled plasmasphere and plasmatrough or depleted outer plasmasphere with steeper density slopes in the latter regions. It is noted that *Goldstein et al.* [2001] and *Denton et al.* [2004] also found a steeper density slope in the plasmatrough. Constrained by the trend of the measured density profiles, we infer the equatorial densities, and extrapolate the density profiles beyond the latitude range of the measured density profiles using the multivariant least squares fit technique, adding to previous efforts in deriving the field-aligned electron density distributions that used limited density measurements approximately made on the same field line [e.g., *Goldstein et al.*, 2001; *Denton et al.*, 2002, 2004]. The empirical model of *Gallagher et al.* [2000] assumed that the plasmasphere and plasmatrough densities were uniformly distributed along the field lines down to the altitude of 1 R_E from the equator, whereas the present study and the previous studies [e.g., *Goldstein et al.*, 2001; *Denton et al.*, 2002, 2004; *Reinisch et al.*, 2001, 2004; *Huang et al.*, 2004] have shown that the electron density profiles at low latitudes (within $\sim 20°$) around the equator is relatively flat with densities still gradually increasing with the distance away from the equator along the field lines.

[25] The equatorial density in the filled flux tubes extrapolated from the multivariant least squares fit to the measured density profiles decreases as L^{-4} (except for the complicated density structure in the 5 November 2004 case), faster than that predicated by the empirical mode of *Carpenter and Anderson* [1992] but consistent with that in the observations of *Reinisch et al.* [2004]. The plasmatrough equatorial density (outer three profiles for 22 March 2001 case) also varies with L^{-4}, slightly slower than that predicted by Carpenter and Anderson model ($N_{eq} \propto L^{-4.5}$) but the same as that in the model of *Sheeley et al.* [2001] and in the observations of *Denton et al.* [2004]. The extrapolated equatorial density of the depleted flux tubes in the outer plasmasphere (outer profiles for the other 2 days), however, decreases with L much faster, approximately $\propto L^{-\gamma}$ with $\gamma \geq 5$. The difference in the L dependence between the extrapolated equatorial density and the empirical model of *Carpenter and Anderson* [1992] may be explained by fluctuations of the individual case observations from the average. In order to obtain the L dependence of the equatorial density under various geophysical and geomagnetic conditions, we need to examine more plasmagrams obtained by the RPI, particularly those with multiple traces. The multiple traces in individual plasmagrams will allow us to derive field-aligned density profiles from one hemisphere to another. Such RPI density profiles will reduce the possible uncertainty of the field line dependence in the equatorial region, including the equatorial densities, associated with the extrapolation of the measured density profiles. So far we have not found plasmagrams obtained by the RPI in the nightside plasmatrough and outer plasmasphere containing multiple traces, although there is plenty of such plasmagrams on the dayside. We are currently investigating why the signals possibly reflected from the conjugate hemisphere are not received by the RPI when the IMAGE is in the low-density nightside plasmatrough and outer plasmasphere.

[26] As suggested by *Higel and Wu* [1984] from GEOS 2 observations at the geosynchronous orbit, the equatorial plasmatrough density around midnight may be at a level as low as 0.1–1 cm^{-3}. The equatorial plasma density presented here is above 8 cm^{-3}. It appears that the RPI has not observed the low-density events suggested by previous observations. *Carpenter and Anderson* [1992] attributed the difficulty to observe such deeply depleted low densities to a possible rapid initial buildup of the plasma from largely unobserved lower "starting" density levels. Note in each case presented in this study, the field line dependence of the densities in the depleted flux tubes can be specified with a common set of parameters. It is possible that the equation (1) also describes common features of the field line dependence of the densities in the deeply depleted flux tubes and thus can be used to specify the plasma density distributions at the start of the plasmasphere refilling, with an equatorial density set to ≤ 0.1 cm^{-3}. In the future, we will further validate the feasibility of empirically modeling the flux tube densities using this functional form through more RPI measurements, i.e., through cases with multiple traces in individual plasmagrams obtained on the nightside. Furthermore, we will study the local time, season, and geomagnetic activity dependence of the fitting parameters with a large set of field-aligned density profiles derived from the RPI sounding measurements so that we will be able to specify the density profiles of the depleted flux tubes under different geomagnetic activities, in different seasons and at various local times.

Finally, we point out that the density distribution given by equation (1) has a density minimum at the equator and hence excludes the possibility of a density peak at the equator, which we have not found any evidence in all the RPI observations we have examined so far.

[27] **Acknowledgments.** This work was supported by NASA under subcontract 83822 from the Southwest Research Institute and by NSF grant NSF-ATM 0518227 to the University of Massachusetts-Lowell. The World Data Center for Geomagnetism (WDC-C2) at Kyoto University, Japan provided the Dst data. The ACE solar wind/IMF data were obtained from the CDAWeb system. We acknowledge the plasmagrams analysis support provided by I. A. Galkin and G. Khmyrov.

[28] Zuyin Pu thanks Richard Denton and another referee for their assistance in evaluating this paper.

References

Angerami, J. J., and D. L. Carpenter (1966), Whistler studies of the plasmapause in the magnetosphere: 2. Electron density and total tube electron content near the knee in magnetospheric ionization, *J. Geophys. Res.*, *71*, 711–725.

Banks, P. M., A. F. Nagy, and W. I. Axford (1971), Dynamical behavior of thermal protons in the mid-latitude ionosphere and magnetosphere, *Planet. Space Sci.*, *19*, 1053–1067.

Benson, R. F., P. A. Webb, J. L. Green, L. Garcia, and B. W. Reinisch (2004), Magnetospheric electron densities inferred from upper-hybrid band emissions, *Geophys. Res. Lett.*, *31*, L20803, doi:10.1029/2004GL020847.

Burch, J. L., et al. (2001), Views of Earth's magnetosphere with the IMAGE satellite, *Science*, *291*, 619.

Carpenter, D. L., and R. R. Anderson (1992), An ISEE/whister model of equatorial electron density in the magnetosphere, *J. Geophys. Res.*, *97*, 1097–1108.

Denton, R. E., J. Goldstein, and J. D. Menietti (2002), Field line dependence of magnetospheric electron density, *Geophys. Res. Lett.*, *29*(24), 2205, doi:10.1029/2002GL015963.

Denton, R. E., J. D. Menietti, J. Goldstein, S. L. Young, and R. R. Anderson (2004), Electron density in the magnetosphere, *J. Geophys. Res.*, *109*, A09215, doi:10.1029/2003JA010245.

Fung, S. F., and J. L. Green (2005), Modeling of field-aligned radio echoes in the plasmasphere, *J. Geophys. Res.*, *110*, A01210, doi:10.1029/2004JA010658.

Gallagher, D. L., P. D. Craven, and R. H. Comfort (2000), Global core plasma model, *J. Geophys. Res.*, *105*, 18,819–18,833.

Goldstein, J., R. E. Denton, M. K. Hudson, E. G. Miftakhova, S. L. Young, J. D. Menietti, and D. L. Gallagher (2001), Latitudinal density dependence of magnetic field lines inferred from Polar plasma wave data, *J. Geophys. Res.*, *106*, 6195–6201.

Green, J. L., and B. W. Reinisch (2003), An overview of results from RPI, *Space Sci. Rev.*, *109*, 183–210.

Higel, B., and L. Wu (1984), Electron density and plasmapause characteristics at 6.6 Earth radii: A statistical study of the GEOS 2 relaxation sounder data, *J. Geophys. Res.*, *89*, 1583–1601.

Horwitz, J. L., R. H. Comfort, and C. R. Chappell (1990), A statistical characterization of plasmasphere density structure and boundary locations, *J. Geophys. Res.*, *95*, 7937–7947.

Huang, X., B. W. Reinisch, P. Song, J. L. Green, and D. L. Gallagher (2004), Developing an empirical density model of the plasmasphere using IMAGE/RPI observations, *Adv. Space Res.*, *33*, 829–833.

Lawrence, D. J., M. F. Thomsen, J. E. Borovsky, and D. J. McComas (1999), Measurements of early and late time plasmasphere refilling as observed from geosynchronous orbit, *J. Geophys. Res.*, *104*, 14,691–14,704.

Liemohn, M. W., G. V. Khazanov, P. D. Craven, and J. U. Kozyra (1999), Nonlinear kinetic modeling of early stage plasmaspheric refilling, *J. Geophys. Res.*, *104*, 10,295–10,306.

Mosier, S. R., M. L. Kaiser, and L. W. Brown (1973), Observations of noise bands associated with the upper hybrid resonance by the IMP 6 radio astronomy experiment, *J. Geophys. Res.*, *78*, 1673–1679.

Rasmussen, C. E., and R. W. Schunk (1988), Multistream hydrodynamic modeling of interhemispheric plasma flow, *J. Geophys. Res.*, *93*, 14,557–14,565.

Reinisch, B. W., et al. (2000), The Radio Plasma Imager investigation on the IMAGE spacecraft, *Space Sci. Rev.*, *91*, 319–359.

Reinisch, B. W., X. Huang, P. Song, G. S. Sales, S. F. Fung, J. L. Green, D. L. Gallagher, and V. M. Vasyliunas (2001), Plasma density distribution along the magnetospheric field: RPI observations from IMAGE, *Geophys. Res. Lett.*, *28*, 4521–4524.

Reinisch, B. W., X. Huang, P. Song, J. L. Green, S. F. Fung, V. M. Vasyliunas, D. L. Gallagher, and B. R. Sandel (2004), Plasmaspheric mass loss and refilling as a result of a magnetic storm, *J. Geophys. Res.*, *109*, A01202, doi:10.1029/2003JA009948.

Sheeley, B. W., M. B. Moldwin, H. K. Rassoul, and R. R. Anderson (2001), An empirical plasmasphere and trough density model: CRRES observations, *J. Geophys. Res.*, *106*, 25,631–25,641.

Singh, N., and J. L. Horwitz (1992), Plasmasphere refilling: Recent observations and modeling, *J. Geophys. Res.*, *97*, 1049–1079.

Singh, N., R. W. Schunk, and H. Thiemann (1986), Temporal features of the refilling of a plasmaspheric flux tube, *J. Geophys. Res.*, *91*, 13,433–13,454.

Sojka, J. J., and G. L. Wrenn (1985), Refilling of geosynchronous flux tubes as observed at the equator by GEOS 2, *J. Geophys. Res.*, *90*, 6379–6385.

Song, P., B. W. Reinisch, and X. Huang (2004), Magnetospheric active wave measurements, *COSPAR Colloq. Ser.*, *16*, 235–246.

Su, Y.-J., M. F. Thomsen, J. E. Borovsky, R. C. Elphic, D. J. Lawrence, and D. J. McComas (2001), Plasmaspheric observations at geosynchronous orbit, *J. Atmos. Sol. Terr. Phys.*, *63*, 1185–1197.

Tsyganenko, N. A. (2002), A model of magnetosphere with a dawn-dusk asymmetry, 2. Parameterization and fitting to observations, *J. Geophys. Res.*, *107*(A7), 1176, doi:10.1029/2001JA000220.

Tu, J.-N., J. L. Horwitz, P. Song, X.-Q. Huang, B. W. Reinisch, and P. G. Richards (2003), Simulating plasmaspheric field-aligned density profiles measured with IMAGE/RPI: Effects of plasmasphere refilling and ion heating, *J. Geophys. Res.*, *108*(A1), 1017, doi:10.1029/2002JA009468.

Wilson, G. R., J. L. Horwitz, and J. Lin (1992), A semikinetic model for early stage plasmasphere refilling: 1. Effects of Coulomb collisions, *J. Geophys. Res.*, *97*, 1109–1119.

J. L. Green, NASA Goddard Space Flight Center, MC 630, Bldg 26, Greenbelt, MD 20771, USA.

X. Huang, B. W. Reinisch, P. Song, and J. Tu, Center for Atmospheric Research, University of Massachusetts-Lowell, 600 Suffolk Street, Lowell, MA 01854, USA. (jiannan_tu@uml.edu)